7-1997

Resuspension and Transport of Fine Sediments by Waves

Chiang C. Mei

She-jun Fan
Old Dominion University

Kang-ren Jin

Original Publication Citation

Mei, C. C., Fan, S. J., & Jin, K. R. (1997). Resuspension and transport of fine sediments by waves. *Journal of Geophysical Research: Oceans, 102*(C7), 15807-15821. doi:10.1029/97jc00584

JOURNAL OF GEOPHYSICAL RESEARCH, VOL. 102, NO. C7, PAGES 15,807–15,821, JULY 15, 1997

Resuspension and transport of fine sediments by waves

Chiang C. Mei

Department of Civil and Environmental Engineering, Massachusetts Institute of Technology Cambridge

She-jun Fan

Department of Ocean Sciences, Old Dominion University, Norfolk, Virginia

Kang-ren Jin

South Florida Water Management District, West Palm Beach

Abstract. Although waves are the primary cause of sediment resuspension in the nearshore zone, in existing theoretical models, long-scale currents induced by the mean wind are often taken to be the only agent for the diffusion and convection of resuspended sediments. We present here theoretical examples where waves play a direct role in all aspects of sediment transport. Details are given for the simple case where only waves are present; the wave-induced current and diffusivity are shown to be no less important than similar factors in the wind-driven current. Hence, in a comprehensive model, one should include not only the current forced directly by the mean wind, but also the current forced by waves which may or may not be forced by the local wind.

Introduction

The subject of resuspension and movement of bottom sediments by fluid flow always has been the central problem of shoreline processes, which is important to coastal engineering and geology. Since sediment deposits and dredged materials in marine environments are also carriers of trace metals, nutrients and other contaminants, there has been intensive interest in recent years in the mathematical modeling of the transport of fine sediments. Models for noncohesive sandy sediments were discussed by *Horikawa* [1988] and *van Rijn* [1994]. For cohesive sediments comprehensive numerical models that account for waves and current generated by wind were developed by *Sheng and Lick* [1979] for Lake Erie. *Sheng* [1984] and his colleagues extended the model for the transport of cohesive sediments and phosphorus in Lake Okeechobee, southern Florida [*Sheng et al.*, 1991; *Shen and Chen*, 1991]. The principal mechanistic ingredients of these models contain two parts. First, the temporal and spatial variation of the current is computed by prescribing the mean wind stress on the water surface. Second, with the computed fluid velocity field, the transport of suspended sediments is then computed from a convection-diffusion equation, subject to an empirical boundary condition on the bed accounting for the erosion and deposition of fine sediments. In both parts, increasingly complex models of turbulence closure have been introduced. The rate of resuspension is usually based on empirical relations expressed in terms of the excess local bed shear above certain thresholds. The role of waves, which is known to be crucial from field observations [*Luettich et al*, 1990; *Sanford*, 1994; *Sheng et al.*, 1991; *Chen and Chen*, 1991], is accounted for only in their contribution to the bed shear stress, which decides the resuspension rate. Typically, wave amplitudes and frequencies are calculated from the local wind velocity or stress via various models such as the simple SMB (Sverdrup-Munk-Bretchneider) model, the JONSWAP (Joint North Sea Wave Project) model, or the more recent WAM (Wave Modeling) model based on radiative transfer theory [*Koman et al*, 1994; *Sobey*, 1986]. The resulting wave field is used to predict bed shear stress, which is added to the current-induced stress for computing the resuspension rate.

While present models have become quite sophisticated in computational and turbulence modeling aspects, they depend on numerous calibration parameters that must be extrapolated from limited field measurements. Many uncertainties not accountable by these turbulence models remain. For example, the bed boundary condition is still based largely on laboratory experiments for steady flows. The dependence of fall velocity on coagulation and flocculation of cohesive sediments, and the effect of consolidation on the threshold stress, are issues that will remain challenging for a long time.

Common in most numerical models, the role of waves is vastly oversimplified. It is known in wave dynamics

Paper number 97JC00584.
0148-0227/97/97JC-00584$09.00

literature that waves also enhance the long-term convection and diffusion of sediments in the wave boundary layer above the bed, where the sediment concentration is the highest. In particular, through second-order Reynolds stresses, waves generate a streaming velocity that varies horizontally on the scale of the wavelength. These velocities may be comparable to the current velocity forced directly by the mean wind stress. For example, the measured current velocity is from 5 to 10 cm/s in the deeper parts of Lake Okeechobee, where waves are of less importance near the bottom, and much smaller near the shore, where wave effects are more pronounced at the bed. For a typical wind, the wave amplitude is 15 cm and the period is 3 s. The first-order orbital velocity is approximately 30 cm/s. The induced streaming velocity near the shallow shore is easily comparable to or greater than the local current induced by the mean wind. Since *Madsen* [1978] showed that such a streaming velocity changes the wind-driven Ekman drift near the surface of a deep sea, similar changes also can be expected near the seabed surface. In addition, *Mei and Chian* demonistrated [1994] that the strong shear in the wave boundary layer also augments the effective diffusion (dispersion) along the sea bottom. Finally, the diurnal variation of wind stress observed over some coasts may also result in long-scale variation of the wave intensity; these variations can, in turn, lead to long waves as a consequence of the second-order radiation stresses forced by the waves.

While a consistent sediment transport model giving due account of both waves and current is needed, we highlight in this paper the multiple roles of waves by simple examples without the mean wind. Using an empirical boundary condition on the seabed, we present an analytical theory for simple harmonic waves over a flat bottom, to examine how waves alone transport fine sediment by convection and diffusion after resuspending them off the bottom.

Formulation

Theories of turbulent wave boundary layers have been constructed on the basis of various semi-empirical and numerical models (eddy viscosity, mixing length, $k-\epsilon$, second-order closure, etc.). Despite differences in detail, models of time-independent eddy viscosity, depth-dependent or constant, do not give substantially different predictions for the ensemble-averaged velocity profile. These models have been extensively surveyed by *Sleath* [1990]. In some experiments [*Jonsson and Carlson*, 1968; *Horikawa*, 1968] there are evidences that the diffusivity depends on time, which can alter the flow qualitatively [*Trowbridge and Madsen*, 1984 a,b]. However, experimental data are relatively scarce for constructing a reliable model. In this paper, we shall adopt the simplest model of constant eddy diffusivity to facilitate analytical results.

Let C denote the volume concentration, $-w_o$ the fall velocity of suspended particles, and D_h, D_v the horizontal and vertical eddy mass diffusivities. The transport equation for the concentration C of a very dilute sediment cloud is

$$\frac{\partial C}{\partial t}+\frac{\partial u_i C}{\partial x_i}+\frac{\partial}{\partial z}\left[(-w_o+w)\,C\right] = D_h\frac{\partial^2 C}{\partial x_i \partial x_i}+D_v\frac{\partial^2 C}{\partial z^2}, \tag{1}$$

where $i=1,2$ with $(x_1,x_2)\equiv(x,y)$ and $(u_1,u_2)\equiv(u,v)$ representing the horizontal coordinates and the fluid velocity components, respectively. The vertical coordinate and velocity component are denoted by z and w. Equation (1) is useful when C is sufficiently small that the presence of the particles does not materially alter the fluid flow.

For a bed of fine and cohesive sediments, experiments in steady and uniform flows have led to the following boundary condition:

$$-D_v\frac{\partial C}{\partial z}-w_o C=-\mathcal{D}+\mathcal{E} \quad z=0. \tag{2}$$

The left-hand side represents the total flux rate in the vertical direction. On the right-hand side, $\mathcal{D}$ stands for the rate of deposition that occurs when the magnitude of the bottom shear stress τ_b is below the threshold τ_d, while $\mathcal{E}$ stands for the rate of erosion (resuspension) that occurs when $|\tau_b|$ is above the threshold τ_c, with $\tau_d<\tau_c$. They are usually given in the following form [*Partheniades*, 1965; *Krone*, 1962]:

$$\mathcal{D} = H(\tau_d-|\tau_b|)w_d C \tag{3}$$

$$\mathcal{E} = H(|\tau_b|-\tau_c)E(|\tau_b|-\tau_c)^m, \tag{4}$$

where $H(x)$ denotes the Heaviside step function of x, w_d is the velocity of deposition and m is some power. The coefficient E depends on the degree of consolidation. For example, for Mississippi Sound sediments $E=10^{-7}$ s/m for 1-day settling to 10^{-8} s/m for 5-day settling, when MKS units are used with $\mathcal{E}$ in kg/m^2 s and τ_b in N/m^2 [*Sheng*, 1984]. Within the range $\tau_d<|\tau_b|<\tau_c$, $\mathcal{D}=\mathcal{E}=0$. The typical value of τ_c is 0.1 N/m^2 in Mississippi Sound. When the bed concentration is significant, w_o and w_d are functions of C. Not enough definitive information is available on the possible relations between the critical shear stresses and various factors such as the sediment size, chemistry, and degree of consolidation; the numerical values found from laboratory or field measurements are usually scattered over a wide range.

The empirical condition (2) is used also for wave-induced sediment transport [*van Rijn*, 1994] where deposition and erosion take place during different parts of the wave cycle. In most estuaries and lakes, the surface layer of the bed is covered by partially consolidated or unconsolidated sediments; the critical shear stress τ_c is usually too small to be measurable by a penetrometer [*Partheniades*, 1965; *Mehta and Partheniades*, 1982; *Mehta*, 1984]. In addition, the wave-induced bed stress of interest can be considerably higher than τ_c, and de-

position can be reasonably ignored altogether. In this paper we shall simplify (2) to

$$-w_o C - D_v \frac{\partial C}{\partial z} = \mathcal{E} = E|\tau_b| \quad z = 0. \tag{5}$$

Modification for the more complex relation (4) is, in principle, straightforward. We shall also take w_o to be a constant to gain mathematical expediency. The inclusion of τ_c and deposition only affects the quantitative prediction without changing the essential features.

Outside the boundary layer we assume

$$C = 0, \qquad z \to \infty. \tag{6}$$

In addition, the initial horizontal distribution of the depth-averaged concentration is prescribed in some source area. Thus the physical problem is to seek the long-term diffusion of a cloud of particles resuspended from a region of erodible bed.

Scaling Estimates

There are three vertical-length scales. One is the thickness of a steady concentration layer due to the balance of gravitational sedimentation and vertical diffusion,

$$\delta_s = \frac{D_v}{w_o}. \tag{7}$$

Associated with fluid oscillations with frequency ω are two other oscillatory boundary layer thicknesses

$$\delta_u = \sqrt{2\nu_e/\omega} \quad \delta_c = \sqrt{2D_v/\omega} \tag{8}$$

corresponding, respectively, to momentum and mass diffusion, where ν_e denotes the eddy viscosity for momentum diffusion. For generality, all three scales are assumed to be comparable, i.e.,

$$O(\delta_s) = O(\delta_u) = O(\delta_c) \tag{9}$$

and the Schmidt number to be of the order of unity

$$Sc = \frac{\nu_e}{D_v} = \left(\frac{\delta_u}{\delta_c}\right)^2 = O(1). \tag{10}$$

We now consider small-amplitude oscillations of high enough frequency that both the wave steepness, kA (k is wave number, A is orbital radius near the seabed) and the ratio of the oscillatory boundary layer thickness to the wave length, $k\delta_u$, are small, i.e.,

$$\epsilon = kA \ll 1 \qquad \beta = k\delta_c\sqrt{\frac{D_h}{D_v}} \ll 1. \tag{11}$$

Assuming for generality that $\epsilon = O(\beta)$, we may introduce the following normalization:

$$x_i^* = kx_i \quad z^* = z/\delta_c \quad t^* = \omega t$$

$$C^* = C/C_o \quad u_i^* = u_i/\omega A \quad w^* = w/k\delta_c\omega A, \tag{12}$$

Equation (6) remains unchanged. The diffusion equation (1) is rescaled to become

$$\frac{\partial C^*}{\partial t^*} + \epsilon\frac{\partial u_i^* C^*}{\partial x_i^*} + \frac{\partial}{\partial z^*}\left[(-Pe + \epsilon w^*)\, C^*\right] = \beta^2\frac{\partial^2 C^*}{\partial x_i^* \partial x_i^*} + \frac{\partial^2 C^*}{\partial z^{*2}}, \tag{13}$$

where $Pe = w_o\delta_c/D_v$ is the Péclet number based on the fall velocity. Again for generality, we assume $Pe \le O(1)$. Now, the period-averaged slow rate of increase of suspended sediment concentration in a unit water column of the wave boundary layer should be balanced by the following mechanisms: horizontal convection by wave-induced streaming, horizontal turbulent diffusion and dispersion, and erosion from the bottom. Accordingly, the scale of the concentration C_o may be estimated by balancing the net rate of horizontal outflux between two cross sections of the bounday layer separated by dx, and the rate of erosion from the bed over the length dx. Let h denote the water depth and τ_o the scale of bottom stress. The convection velocity due to wave-induced mass transport should be of the order of

$$u = O(kAU_b) \sim kA\frac{A}{h}\sqrt{gh} \tag{14}$$

where the bottom orbital velocity is estimated for long waves

$$U_b = \frac{A}{h}\sqrt{gh}. \tag{15}$$

The scale C_o can then be estimated according to the following balance of terms,

$$\delta_c u\frac{\partial C}{\partial x}\, dx \sim E\tau_o\, dx,$$

or, equivalently, the following balance of scales,

$$\delta_c k^2 A^2\sqrt{\frac{g}{h}}C_o \sim E\tau_b \sim \rho E D_v\frac{A\sqrt{gh}}{\delta_c h},$$

where the bottom stress is estimated from the model of constant eddy viscosity

$$\tau_o = \frac{\sqrt{2}\rho D_v U_b}{\delta_c} = \frac{\sqrt{2}\rho D_v A\sqrt{g}}{\delta_c\sqrt{h}} \tag{16}$$

Therefore the scale of concentration C_o is of the order of

$$C_o \sim \frac{2\sqrt{2}\rho E D_v}{k^2\delta_c^2 A}. \tag{17}$$

Note that C_o is independent of the fall velocity and hence of the particle size. But C_o depends on the eddy viscosity, and hence, on bed roughness and the flow velocity.

To have some quantitative idea of the scales, let us take the typical data for Lake Okeechobee with $\omega = 2\pi/3$ rad/s, $A = 0.1$ m, $h = 3$ m, so that $k = \omega/\sqrt{gh} = 0.3823$ m^{-1} and $U_b = 0.18$ m/s. Taking a range $2 \times 10^{-4} < D_v < 20 \times 10^{-4}$ m^2/s, we get $0.01447 < \delta_c =$

0.04576 m. It follows from (16) that $1.784 < \tau_o < 11.28$ N/m^2. For reference the bottom shear stress due to wind-driven current alone is typically only 0.3 N/m^2 [*Sheng and Cook*,1990]. For later reference, we compute C_o by taking $E = 5.5 \times 10^{-9}$s/m which is the value used by *Sheng and Cook* [1990, equation (2-19), p. 2-22]. It follows readily from (17) that $C_o = 0.821 \times 10^{-5}$ kg/m^3 $= 0.821 \times 10^{-2}$ mg/L.

The boundary condition (5) may now be normalized to

$$-PeC' - \frac{\partial C'}{\partial z'} = \frac{k\delta_c^2 U_b^2}{\omega D_v}|\tau_b'|, \tag{18}$$

where $\tau_b' = \tau_b/\tau_o$ and

$$\frac{k\delta_c^2 U_b^2}{\omega D_v} = O(kA)^2 = O(\epsilon^2). \tag{19}$$

Since Pe is at most of the order of unity, the above result implies that the erosion rate is smaller than the flux terms on the left-hand side by a factor of the order $O(\epsilon^2)$. The preceding order estimate of (19) made by heuristic theoretical reasoning is crucial to later analysis, hence support by field observation is desirable.

During the period from 1128 to 1855, the Yellow River of China entered the Pacific Ocean through the Huai River Estuary on the northern coast of Jian Su Province. Frequent floods and sediment deposits resulted in a large delta. Since 1885, the Yellow River mouth has moved to the Po-Hai seacoast of Shantung Province, north of Jian Su. In the delta region of the old Yellow River mouth, where cohesive sediments dominate, the sediment dynamics is largely the result of local waves and tidal currents. Continuous erosion in the last century has deepened the submerged part of the delta, providing good natural conditions for a deep harbor. For this and other economical reasons extensive field surveys have been conducted by the State Key Laboratory of Estuarine and Coastal Research, East China Normal University, Shanghai and the Lianyungong Harbor Port Authority. In particular, from records during 1956-1982, the coastline retreats at the average annual rate of 26-50 m/yr [*Yu* , 1993]. The average slope being 1/500 $\sim$ 1/1000, the coastal depth increases at the rate of 2.6 $\sim$ 10 cm/yr. Estimating the density of the muddy seabed at 1650 kg/m^3, the average rate of erosion is $\mathcal{E} = 1.36 \times 10^{-6} \sim 5.23 \times 10^{-6}$ kg/m^2 s. The typical fall velocity of very fine sediments is approximately $w_o = 0.028$ cm/s [*Huhe and Yang*, 1996]. During May 1988, sediment concentration was measured from boats at eight stations in depths ranging from 2 m to 12 m [*Yu*, 1993]. Based on depth-averaged concentration $\overline{C}$, the ratio of erosion to a typical flux term, $\mathcal{E}/w_o\overline{C}$, is calculated in Table 1. We have included the recorded tidal velocity u_T which can be used to estimate the tidal amplitude A_T by the long wave theory, $A_T = u_T\sqrt{h/g}$.

From the statistical information on wave climate for July 1993 to June 1994, $H_{1/10}$ exceeds 1 m at the frequency of 22.4%, and 3 m at the frequency of 1.45%; the typical peak period is in the range of 8.1 - 8.5 s. While these wave data are lacking in detail, the smallness of the observed $\mathcal{E}/w_o\overline{C}$ clearly supports the order estimate in (19).

Effective Transport Equation by Multiple-Scale Expansions

Having identified the orders we return to the dimensional form (1) by inserting an ordering parameter ϵ as follows:

$$\frac{\partial C}{\partial t} + \epsilon\frac{\partial u_i C}{\partial x_i} + \frac{\partial}{\partial z}\left[(-w_o + \epsilon w)\, C\right] = \epsilon^2 D_h \frac{\partial^2 C}{\partial x_i \partial x_i} + D_v \frac{\partial^2 C}{\partial z^2}, \tag{20}$$

$$-w_o C - D_v\frac{\partial C}{\partial z} = \epsilon^2 E|\tau_b| \quad z = 0. \tag{21}$$

In the convection-diffusion process, there are two distinct time-scales corresponding to the contrasting ver-

Table 1. Ratio of Erosion to Flux terms

		Strong tide, May 5-6, 1993			
Station	1	2	3	6	7
Depth, m	6.6	10.3	12.2	5.7	12.8
Speed, m/s		-0.62$\sim$ 0.63	-0.72$\sim$ 0.64	-0.53$\sim$ 0.61	
$\overline{C}$, kg/m^3	0.99	0.69	0.63	0.92	0.65
$\mathcal{E}/w_o\overline{C}$	0.005$\sim$ 0.019	0.007 $\sim$ 0.027	0.008$\sim$ 0.030	0.005$\sim$ 0.020	0.007 $\sim$ 0.029
		Medium tide, May 9-10, 1993			
Station	1	2	3	4	5
Depth, m	6.6	10.3	12.2	4.0	11.5
Speed, m/s	-0.60$\sim$ 0.53	-0.70$\sim$ 0.65	-0.64$\sim$ 0.59		
$\overline{C}$, kg/m^3	1.32	0.89	0.61	0.81	0.61
$\mathcal{E}/w_o\overline{C}$	0.004$\sim$ 0.014	0.005$\sim$ 0.020	0.008$\sim$ 0.031	0.006$\sim$ 0.023	0.008 $\sim$ 0.031
		Weak tide , May15-16, 1993			
Station	1	2	3	4	5
Depth, m	6.6	10.3	12.2	5.7	10
Speed, m/s	-0.48$\sim$ 0.38	-0.54$\sim$ 0.47	-0.44$\sim$ 0.41	-0.28$\sim$ 0.33	-0.49$\sim$
$\overline{C}$, kg/m^3	0.62	0.58	0.43	049	0.76
$\mathcal{E}/w_o\overline{C}$	0.008$\sim$ 0.031	0.008$\sim$ 0.032	0.011$\sim$ 0.043	0.010 $\sim$ 0.038	0.006 $\sim$ 0.025

tical and horizontal length scales. These are the diffusion time across a boundary layer, which is the same as a wave period, $O(\omega^{-1}) = O(\delta^2/D_v)$, and the diffusion time across a wave length, $O(1/k^2 D_h)$. The ratio between the two is $O(k^2\delta^2(D_h/D_v)) \equiv O(\beta^2)$. Under the assumption $\epsilon = O(\beta)$, we shall introduce two time variables: t and $T = \epsilon^2 t$. The velocity and concentration are expanded as follows:

$$u_i = u_i^{(1)} + \epsilon u_i^{(2)} + O(\epsilon^2) \quad (22)$$

$$w = w^{(1)} + \epsilon w^{(2)} + O(\epsilon^3) \quad (23)$$

$$C = C^{(0)} + \epsilon C^{(1)} + \epsilon^2 C^{(2)} + O(\epsilon^3), \quad (24)$$

where $u_i^{(n)}$ and $w^{(n)}$ are functions of x_i, z and t and $C^{(n)} = C^{(n)}(x_i, z, t, T)$. For the sake of clarity, we follow *Mei and Chian* [1994] and sketch the derivation of the governing equation for $C^{(0)}$.

Focusing attention on the physics beyond the initial transient of a few wave periods, we consider only the long time evolution of the bed concentration. Hence $C^{(0)}(x_i, z, T)$ depends not on the fast time t but only on T and is governed by a homogeneous differential equation in z

$$-w_o \frac{\partial C^{(0)}}{\partial z} = D_v \frac{\partial^2 C^{(0)}}{\partial z^2} \qquad 0 < z < \infty. \quad (25)$$

The homogeneous boundary conditions are

$$w_o C^{(0)} + D_v \frac{\partial C^{(0)}}{\partial z} = 0 \qquad z = 0 \quad (26)$$

and

$$C^{(0)} = 0 \qquad z \to \infty. \quad (27)$$

Thus, a nontrivial solution exists

$$C^{(0)} = \widehat{C}(x_i, T)\mathcal{F}(z), \quad (28)$$

where

$$\mathcal{F}(z) = \exp\left(-\frac{w_o z}{D_v}\right) \quad (29)$$

and $\widehat{C}$ is the leading-order concentration at the seabed.

At $O(\epsilon)$, $C^{(1)}$ represents the perturbation due to the oscillating velocity field and satisfies

$$\frac{\partial C^{(1)}}{\partial t} - w_o \frac{\partial C^{(1)}}{\partial z} - D_v \frac{\partial^2 C^{(1)}}{\partial z^2} = -\frac{\partial (u_i^{(1)} C^{(0)})}{\partial x_i} - \frac{\partial (w^{(1)} C^{(0)})}{\partial z} \quad (30)$$

and the boundary conditions

$$w_o C^{(1)} + D_v \frac{\partial C^{(1)}}{\partial z} = 0 \qquad z = 0 \quad (31)$$

and

$$C^{(1)} = 0 \qquad z \to \infty. \quad (32)$$

At $O(\epsilon^2)$, $C^{(2)}$ satisfies

$$\frac{\partial C^{(2)}}{\partial t} - w_o \frac{\partial C^{(2)}}{\partial z} - D_v \frac{\partial^2 C^{(2)}}{\partial z^2} = -\frac{\partial C^{(0)}}{\partial T} - \frac{\partial u_i^{(1)} C^{(1)}}{\partial x_i} - \frac{\partial w^{(1)} C^{(1)}}{\partial z} - \frac{\partial u_i^{(2)} C^{(0)}}{\partial x_i} - \frac{\partial w^{(2)} C^{(0)}}{\partial z} + D_h \frac{\partial^2 C^{(0)}}{\partial x_j \partial x_j} \quad (33)$$

and the boundary conditions

$$-w_o C^{(2)} - D_v \frac{\partial C^{(2)}}{\partial z} = E|\tau_b| \qquad z = 0 \quad (34)$$

and

$$C^{(2)} = 0 \qquad z \to \infty. \quad (35)$$

Our interest is in the slow diffusion at the leading order, and attention will be focused on the governing equation for the bed concentration $\widehat{C}(x_i, T)$, defined by (28).

Let the wave velocity at the leading order $(u_i^{(1)}, w^{(1)})$ be simple harmonic in time with the frequency ω. All the forcing terms on the right of (30) are then simple harmonic in the fast time t. Let the period-average (time average with respect to a wave period) of any quantity f be denoted by $\bar{f}$. Then $\bar{C}^{(1)}$ is governed by the same homogeneous conditions (25), (31) and (32) as $C^{(0)}$, and hence can be discarded without loss of generality. Then $C^{(1)}$ consists only of first harmonic fluctuations

$$C^{(1)} = \Re\left(C_{11} e^{-i\omega t}\right), \quad (36)$$

where $C_{11} = C_{11}(x_i, z, T)$ and $\Re$ denotes the real part of its argument. Taking the time-average of (33) - (35) over the wave period, we find that $\bar{C}^{(2)}$ satisfies an inhomogeneous differential equation similar to (4.6), the boundary conditions

$$-w_0 \bar{C}^{(2)} - D_v \frac{\partial \bar{C}^{(2)}}{\partial z} = E\overline{|\tau_b|}, \quad (37)$$

and (27). Let the vertical integration of $f(z)$ across the entire boundary layer be denoted by $\langle f(z)\rangle$, then the depth average of the inhomogeneous boundary-value problem for $\bar{C}^{(2)}$ is

$$\frac{\partial \widehat{C}}{\partial T} + \frac{1}{\delta_s}\frac{\partial \left[\langle \bar{u}_i^{(2)} \mathcal{F}\rangle \widehat{C}\right]}{\partial x_i} = -\frac{1}{\delta_s}\frac{\partial \langle \overline{u_i^{(1)} C^{(1)}}\rangle}{\partial x_i} + D_h \frac{\partial^2 \widehat{C}}{\partial x_j \partial x_j} + \frac{E\overline{|\tau_b|}}{\delta_s}, \quad (38)$$

where use has been made of (28) and (29). This transport equation is an extension of *Mei and Chian* [1994] who ignored resuspension. The only difference is the last source term representing erosion. A similar equation was used previously for erosion in steady river streams [van Rijn, 1994].

Mei and Chian have shown that $\bar{u}^{(2)}$ represents the second-order Eulerian streaming induced by Reynolds

stresses. The first term on the right-hand side of (38) is the result of convection by the first-order oscillatory velocity, leading to an apparent diffusion analogous to Taylor dispersion. The second term represents horizontal diffusion due directly to turbulence. Let the leading-order inviscid flow velocities above the boundary layer be given by

$$U_i = \Re\left(U_{oi}e^{-i\omega t}\right), \tag{39}$$

where $U_{oi} = U_{oi}(x_j)$ is the spatial amplitude of U_i. Eq. (38) then becomes

$$\frac{\partial \widehat{C}}{\partial T} + \frac{\partial}{\partial x_i}\left(\mathcal{U}_i\widehat{C}\right) = D_h\frac{\partial^2\widehat{C}}{\partial x_j\partial x_j} + \frac{\partial}{\partial x_i}\left(\mathcal{D}_{ij}\frac{\partial \widehat{C}}{\partial x_j}\right) + \frac{E\overline{|\tau_b|}}{\delta_s} \tag{40}$$

where $\mathcal{U}, \mathcal{V}$ and $\mathcal{D}_{ij}$ can be found in terms of U_{oi}. Specifically,

$$\mathcal{U} = \frac{1}{\omega}\Re\left(H_1U_o\frac{\partial U_o^*}{\partial x} + H_2V_o\frac{\partial U_o^*}{\partial y} + H_3U_o\frac{\partial V_o^*}{\partial y}\right) \tag{41}$$

$$\mathcal{V} = \frac{1}{\omega}\left(H_1V_o\frac{\partial V_o^*}{\partial y} + H_2U_o\frac{\partial V_o^*}{\partial x} + H_3V_o\frac{\partial U_o^*}{\partial x}\right) \tag{42}$$

$$\begin{pmatrix}\mathcal{D}_{xx}\\ \mathcal{D}_{xy}\\ \mathcal{D}_{yx}\\ \mathcal{D}_{yy}\end{pmatrix} = \Re\frac{H_4}{\omega}\begin{pmatrix}|U_o|^2\\ U_oV_o^*\\ U_o^*V_o\\ |V_o|^2\end{pmatrix} \tag{43}$$

where $\mathcal{U}$ and $\mathcal{V}$ are the components of weighted depth-average of Eulerian streaming. The tensor $\mathcal{D}_{ij}$ arises from the correlations $\langle u_i^{(1)}C^{(1)}\rangle$. The coefficients $H_n, n = 1, 2, 3, 4\ldots$, have been derived in explicit form and plotted by *Mei and Chian* [1994] as functions of Pe and Sc. In particular, H_4 is complex; hence the tensor E_{ij} is in general not symmetric, i.e., $\mathcal{D}_{ij} \neq \mathcal{D}_{ji}$.

The source term on the right of (40) represents the mean rate of erosion averaged over a wave period, and can be computed from the local stress at the bed

$$\begin{pmatrix}\tau_{bx}\\ \tau_{by}\end{pmatrix} = \frac{\sqrt{2}\rho\nu_e}{\delta_u}\Re\left[\begin{pmatrix}U_0(x,y)\\ V_0(x,y)\end{pmatrix}e^{-i(\omega t+\frac{\pi}{4})}\right] \tag{44}$$

The formulas deduced here are general for small amplitude waves of any spatial variation as long as the first-order inviscid velocity (U_o, V_o) in the tangential direction is known at the upper edge of the boundary layer.

On a cliff-like coast the normal flux will be required to vanish, i.e.,

$$n_i\left(\mathcal{U}_i\widehat{C} - (\mathcal{D}_{ij} + D_h\delta_{ij})\frac{\partial \widehat{C}}{\partial x_j}\right) = 0. \tag{45}$$

where $\{n_i\}$ denotes the unit normal to the coast line.

We now consider several examples to examine the effects of the wave pattern and the geometry of the erodible bed. In all numerical illustrations, we choose $D_h = D_v = \nu_e = D$ and $Pe = 1$, implying that $Sc = 1$ and $\delta_s = \delta_c = \delta_u = \delta$. For these inputs it can be found from *Mei and Chian* [1994] that

$$\begin{aligned} H_1 &= -0.122058 + 0.659452\,i,\\ H_2 &= 0.033333\\ H_3 &= -0.155391 + 0.659452\,i,\\ H_4 &= 0.023615 + 0.233866\,i. \end{aligned} \tag{46}$$

Progressive Waves Over an Erodible Patch

We first study a one-dimensional example where a train of progressive waves passes normally over an strip of erodible bed of width L in the cross-shore direction $(0 < x < L)$ and infinitely long in the longshore direction. Ignoring viscous attenuation, the inviscid velocity near the seabed is

$$u^{(1)} = \Re(U_0(x)e^{-i\omega t}) = \Re(U_be^{ikx}e^{-i\omega t}), \tag{47}$$

where $\omega = k\sqrt{gh}$ and $U_b = (A/h)\sqrt{gh}$ for long waves in shallow water. We stress that this theory can be applied to internal waves with minor modifications. From Stokes theory of oscillatory boundary layers, the bed shear stress is

$$\tau_b = \frac{\sqrt{2}\rho D}{\delta}\Re\left[U_0(x)e^{-i(\omega t+\pi/4)}\right]. \tag{48}$$

The time-averaged erosion rate is

$$E\overline{|\tau_b|} = \frac{2\sqrt{2}\rho D_v M U_b}{\pi\delta}, \tag{49}$$

which is constant in x. By using the following normalized variables (with primes)

$$x' = kx \quad T' = \frac{k^2U_b^2}{\omega}T \quad U_0' = \frac{U_o}{U_b} \quad \widehat{C}' = \frac{\widehat{C}}{C_o}, \tag{50}$$

where C_o is defined by (17), and the normalized coefficients

$$\begin{aligned} \mathcal{U}' &= \frac{\mathcal{U}\omega}{kU_b^2} = \Im(H_1) \quad D' = \frac{D\omega}{U_b^2}\\ \mathcal{D}_{xx}' &= \frac{\mathcal{D}_{xx}\omega}{U_b^2} = \Re(H_4), \end{aligned} \tag{51}$$

we get

$$\frac{\partial \widehat{C}'}{\partial T'} + \frac{\partial \mathcal{U}'\widehat{C}'}{\partial x'} = K'\frac{\partial^2\widehat{C}'}{\partial x'^2} + \mathcal{E}'(x'), \tag{52}$$

where

$$K' = D' + \mathcal{D}_{xx}' \qquad \mathcal{E}'(x') = \begin{cases} 1 & 0 < x' < L' = kL\\ 0 & x' < 0, x' > L' \end{cases} \tag{53}$$

The problem can be solved analytically by Fourier transform in terms of error functions

$$\widehat{C}' = \frac{1}{2}\int_0^{T'} d\tau \left[\text{erf}\left(\frac{x' - \mathcal{U}'(T'-\tau)}{2\sqrt{K'(T'-\tau)}}\right) - \text{erf}\left(\frac{x' - L' - \mathcal{U}'(T'-\tau)}{2\sqrt{K'(T'-\tau)}}\right)\right]. \quad (54)$$

The analytical solution is plotted in Figure 1 for $\mathcal{U}' = 0.659452, \mathcal{D}'_{xx} = 0.023615$ in accordance with (46), and for $D' = 0.001$ and $L' = 2\pi$. At the initial stage, the bottom sediment concentration increases just above the erodible strip. The stern of the sediment cloud is convected forward. The front of the cloud is stretched in the direction of wave propagation. After a long enough time, a steady state is reached over the erodible part where

$$\hat{C}' = \begin{cases} \frac{x'}{\mathcal{U}'} + \frac{K'}{\mathcal{U}'^2} e^{-\frac{\mathcal{U}'L'}{K'}}\left(1 - e^{\frac{\mathcal{U}'x'}{K'}}\right), & x' \in (0, L') \\ \frac{L'}{\mathcal{U}'} - \frac{K'}{\mathcal{U}'^2}\left(1 - e^{-\frac{\mathcal{U}'L'}{K'}}\right), & x' > L'. \end{cases} \quad (55)$$

In the numerical example, $K/\mathcal{U}^2 = 0.0566 \ll 1$, so that the steady state limit is dominated by the first term on the right-hand side in the preceding equation. As the front moves further across the nonerodible part, a steady state is also reached at the back with constant concentration. This steady state is possible only if the erodible strip has an unlimited supply of sediments and the waves remain undiminished; both conditions are idealizations of reality. Also, the steady state concentration is larger for a larger L' or a smaller $\mathcal{U}'$. Note that the timescale to reach steady state is inversely proportional to U_b^2. Hence for weaker waves, the steady state is more remote. For the example of Lake Okeechobee, the timescale of advection is $\omega/k^2U_b^2 = 30.44$ s; the corresponding time to reach steady state is 10 times this scale, as shown in Figure 1, or 5 min =100 wave periods. Such a short time is the consequence of neglecting wind-driven current in which vertical diffusion across the entire lake depth would greatly delay the process toward the steady state.

Much of the eastern part of the the bottom of Lake Okeechobee is covered by mud at depths up to 0.85 m.

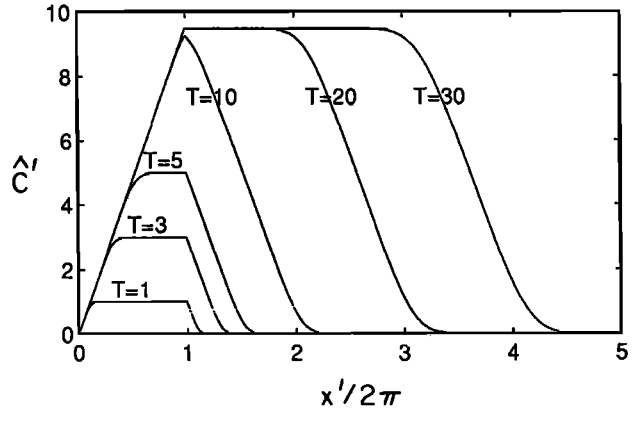

Figure 1. Bottom concentration due to normally incident waves over an erodible strip $0 < x'/2\pi < 1$.

As an order estimate, let $L' = 2\pi \times 10^3$ corresponding to an erodible strip of width equal to 1000 wavelngths or 16 km . The maximum bottom concentration calculated from (55) is

$$C_o\frac{L'}{\mathcal{U}'} = 0.07822\frac{\text{kg}}{\text{m}^3} = 78.22\,\frac{\text{mg}}{\text{L}} \quad (56)$$

As a comparsion, the maximum concentration measured at Station C near the center of Lake Okeechobee is 0.03 - 0.10 kg/m^3= 20-100 mg/L. These magnitudes are consitent with the theoretical estimate of (56) . Not included in the present theory, wind-driven current exists far above the wave boundary layer and should help the distribution of resuspended sediments at much greater height.

We remark that there are one-dimensional models involving wind and waves [*Luettich et al*, 1990; *Sheng and Cook*, 1990], where horizontal advection due to the mean wind is assumed to affect only the turbulent diffusivity and the bottom friction. Suspended sediments are only diffused upward but not advected horizontally by the current. Such a model is appropriate if there is horizontal uniformity, corresponding approximately to the center part of a very large area of erosion, and for episodic events lasting a few days. In our example, sediments are transported only in the very thin wave boundary layer. Vertical diffusion is complete within a few wave periods, and horizontal advection must take place, because there is no horizontal uniformity due to the finite length of waves. Indeed without horizontal advection and diffusion, a steady state limit involving only vertical diffusion is not possible, as can be seen from (52).

We next present the results for a square patch of erodible bed, $0 < x' < 2\pi, -\pi < y' < \pi$. Now the governing equation is changed to

$$\frac{\partial \widehat{C}'}{\partial t'} + \frac{\partial \mathcal{U}'\widehat{C}'}{\partial x} = (D' + \mathcal{D}'_{xx})\frac{\partial^2 \widehat{C}'}{\partial x'^2} + D'\frac{\partial \widehat{C}'}{\partial y^2} + \mathcal{E}'(x', y'), \quad (57)$$

where

$$\mathcal{E}'(x', y') = \begin{cases} 1 & x' \in (0, 2\pi),\ y' \in (-\pi, \pi) \\ 0 & x' \notin (0, 2\pi),\ y' \notin (-\pi, \pi). \end{cases} \quad (58)$$

Although an analytical solution is possible, a numerical solution by the finite differences method of alternating directions is also straightforward. Figure 2 shows the evolution of concentration contours in time. The concentration cloud starts from the patch and grows to a rectangular plateau with rounded corners. The front of the plateau extends with time in the direction of wave propagation, while the rear is also convected forward. The lateral expansion is slower because of the smaller combined diffusivity. For large enough time, a finite height is reached near the stern of the plateau. As expected, the bed concentration along the x axis evolves in the same way as in the one-dimensional example.

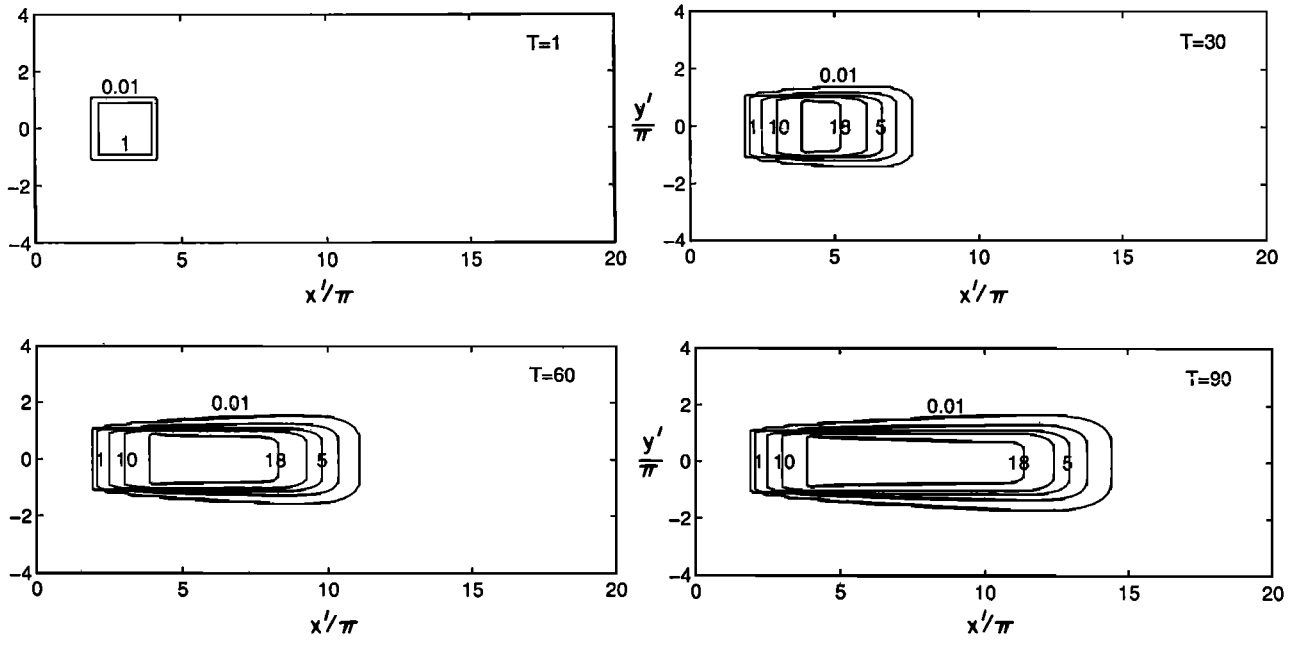

Figure 2. Bottom concentration contours due to waves passing an erodible square.

Waves Reflected From a Seawall

Let the y axis coincide with the vertical seawall toward which a train of monochromatic surface waves of long period is incident and reflected obliquely. The surface wave displacement is

$$\zeta = 2A\cos(kx\cos\theta)e^{i(ky\sin\theta-\omega t)}. \tag{59}$$

where A denotes the amplitude of the long wave. The inviscid velocity components near the seabed are

$$U_0 = 2iU_b\cos\theta\sin(kx\cos\theta)e^{ky\sin\theta} \tag{60}$$

and

$$V_o = 2U_b\sin\theta\cos(kx\cos\theta)e^{iky\sin\theta}, \tag{61}$$

where U_b is still defined by (15).

Normalized according to (50), the coefficients in the dispersion equation read [*Mei and Chian*, 1994]

$$\mathcal{U}' = \{2\Re(H_1)\cos^3\theta + [\Re(H_3) - \Re(H_2)] \cdot \sin\theta\sin(2\theta)\}\sin(2x'\cos\theta) \tag{62}$$

$$\mathcal{D}'_{xx} = 4\Re(H_4)\cos^2\theta\sin^2(x'\cos\theta). \tag{63}$$

The erosion rate on the right-hand side of (40) becomes

$$E\overline{|\tau_b|} = \frac{\delta k^2U_b^2C_o}{2\omega}\int_0^{2\pi}[a^2+(b^2-a^2)\cos^2\psi]^{1/2}d\psi, \tag{64}$$

where

$$a = \cos\theta\sin(x'\cos\theta),\ b = \sin\theta\cos(x'\cos\theta) \tag{65}$$

and C_o is defined by

$$C_o = \frac{2\sqrt{2}\rho ED\omega}{\pi k^2\delta^2U_b} = \frac{2\sqrt{2}\rho ED}{\pi k^2\delta^2A} \tag{66}$$

Except for a factor 2π, (66) is consistent with (17) since $U_b = \omega A$. Because all coefficients in the transport equation as well as the forcing term are independent of y, $\widehat{C}'$ is governed by the one-dimensional equation

$$\frac{\partial\widehat{C}'}{\partial t'} + \frac{\partial\mathcal{U}'\widehat{C}'}{\partial x} = K'_{xx}\frac{\partial^2\widehat{C}'}{\partial x'^2} + \mathcal{E}'(x'), \tag{67}$$

where $K'_{xx} = D' + \mathcal{D}'_{xx}$ and

$$\mathcal{E}'(x') = \frac{1}{2}\int_0^{2\pi}[a^2 + (b^2 - a^2)\cos^2\psi]^{1/2}d\psi \tag{68}$$

for $x' \in (0, L')$ and zero elsewhere. From (62) and (63) $\mathcal{U}'$ and K_{xx} vary periodically in x', as shown in Figure 3a for $\theta = \pi/4$. Zeroes in the convection field coincide with the minima of the dispersion coefficient. Thus, sediments are convected toward the lines $2x'\cos\theta = n\pi$ where diffusion is the weakest. Figure 3b shows a normalized erosion rate and Figure 4 shows the bottom concentration distribution when the erodible area is a strip $0 < x' < 4\pi$ along the seawall. Clearly, sediments tend to accumulate over the lines toward which the convection velocity converges.

Standing Waves in a Rectangular Lake

Let us examine the transport in the bottom boundary layer beneath a long standing wave in a rectangular lake. For simplicity, we treat the simplified case where waves are unattenuated either by ignoring frictional damping after the passage of wind, or by assuming that the tendency for wave growth is exactly counterbalanced by damping. Let the basin have the depth h, width a, and length b. The free-surface displacement of the seiche mode is assumed to be

$$\zeta = A\cos\frac{m\pi x}{a}\cos\frac{n\pi y}{b}e^{-i\omega t}, \tag{69}$$

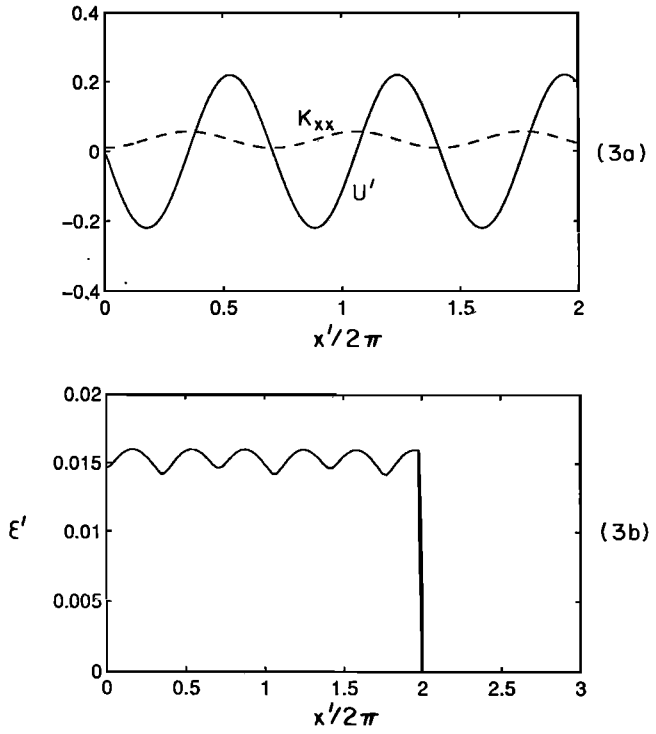

Figure 3. Waves reflected from a seawall with angle of incidence $\theta = 45°$. (a) Total diffusivity K'_{xx} and effective convection velocity U'. (b) Erosion rate.

where A is the constant amplitude. The eigenfrequency is

$$\omega = \left[gh\left(\frac{m^2\pi^2}{a^2} + \frac{n^2\pi^2}{b^2}\right)\right]^{1/2} \tag{70}$$

The amplitudes of the free stream velocities are then given by

$$U_o = \frac{imU_b\sqrt{a^2+b^2}}{a} \sin\frac{m\pi x}{a} \cos\frac{n\pi y}{b} \tag{71}$$

and

$$V_o = \frac{inU_b\sqrt{a^2+b^2}}{b} \cos\frac{m\pi x}{a} \sin\frac{n\pi y}{b}, \tag{72}$$

where U_b is refined as

$$U_b = \frac{\pi g A}{\omega} \frac{1}{\sqrt{a^2+b^2}} \tag{73}$$

Let us introduce the normalization

$$x' = \frac{\pi x}{a} \quad y' = \frac{\pi y}{b} \quad U'_o = \frac{U_o}{U_b} \quad V'_o = \frac{V_o}{U_b}. \tag{74}$$

We get in dimensionless form

$$\begin{aligned} U'_o &= i\sqrt{1+s^2}\sin mx'\cos ny' \\ V'_o &= i\sqrt{1+s^{-2}}\cos mx'\sin ny', \end{aligned} \tag{75}$$

where s denotes the aspect ratio

$$s \equiv \frac{b}{a}. \tag{76}$$

The resulting coefficients are, in dimensionless form,

$$\mathcal{U}' = \frac{1}{2}\Re\left[(m^3(1+s^2)H_1 + mn^2(1+s^{-2})H_3)\cos^2 ny' - mn^2(1+s^{-2})H_2\sin^2 ny'\right]\sin 2mx' \tag{77}$$

and

$$\mathcal{V}' = \frac{1}{2s^2}\Re\left[(n^3(1+s^{-2})H_1 + m^2n(1+s^2)H_3)\cos^2 mx' - m^2n(1+s^2)H_2\sin^2 mx'\right]\sin 2ny', \tag{78}$$

which are the corrected versions of (6.6) in the work by *Mei and Chian* [1994].

In this case $\mathcal{D}'_{ij}$ is symmetric since the tensor $U'^*_{oi}U'_{oj}$ is real, and

$$\mathcal{D}'_{xx} = \Re(H_4)m^2(1+s^2)\sin^2 mx'\cos^2 ny', \tag{79}$$

$$\mathcal{D}'_{yy} = \Re(H_4)n^2s^{-2}(1+s^{-2})\cos^2 mx'\sin^2 ny', \tag{80}$$

$$\mathcal{D}'_{xy} = \mathcal{D}'_{yx} = \frac{\Re(H_4)}{4}mn(1+s^{-2})\sin 2mx'\sin 2ny'. \tag{81}$$

With the first-order velocity scale given by (73), the physical bottom shear stress components are

$$\begin{pmatrix} \tau_{bx} \\ \tau_{by} \end{pmatrix} = \frac{\sqrt{2}\rho D}{\delta} U_b\sqrt{a^2+b^2}\sin(\omega t + \frac{\pi}{4}) \cdot \begin{pmatrix} \frac{m}{a}\sin\frac{m\pi x}{a}\cos\frac{n\pi y}{b} \\ \frac{n}{b}\cos\frac{m\pi x}{a}\sin\frac{n\pi y}{b} \end{pmatrix}. \tag{82}$$

The dimensionless averaged erosion rate is

$$\mathcal{E}'(x',y') = \frac{\overline{|\tau_b|}}{\tau_o} = \left[m^2(1+s^2)\sin^2 mx'\cos^2 ny' + n^2(1+s^{-2})\cos^2 mx'\sin^2 ny'\right]^{1/2}, \tag{83}$$

where

$$\tau_o = \frac{2\sqrt{2}\rho D U_b}{\pi\delta}. \tag{84}$$

We now consider two rectangular lakes A and B with identical dimensions (a, b). In Lake A the coastal belt is erodible; the normalized width of the belt is $\pi/4$. In Lake B, only a rectangular area at the lake cen-

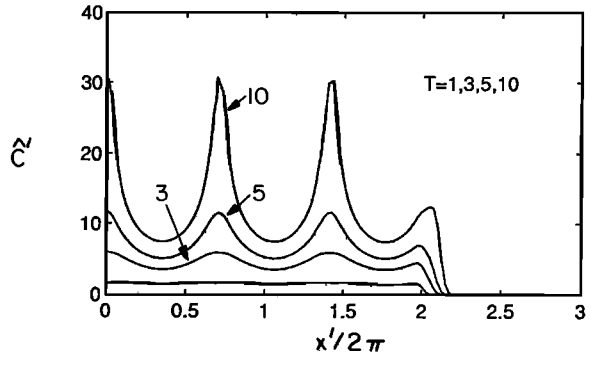

Figure 4. Bottom concentration due to wave reflection from a wall.

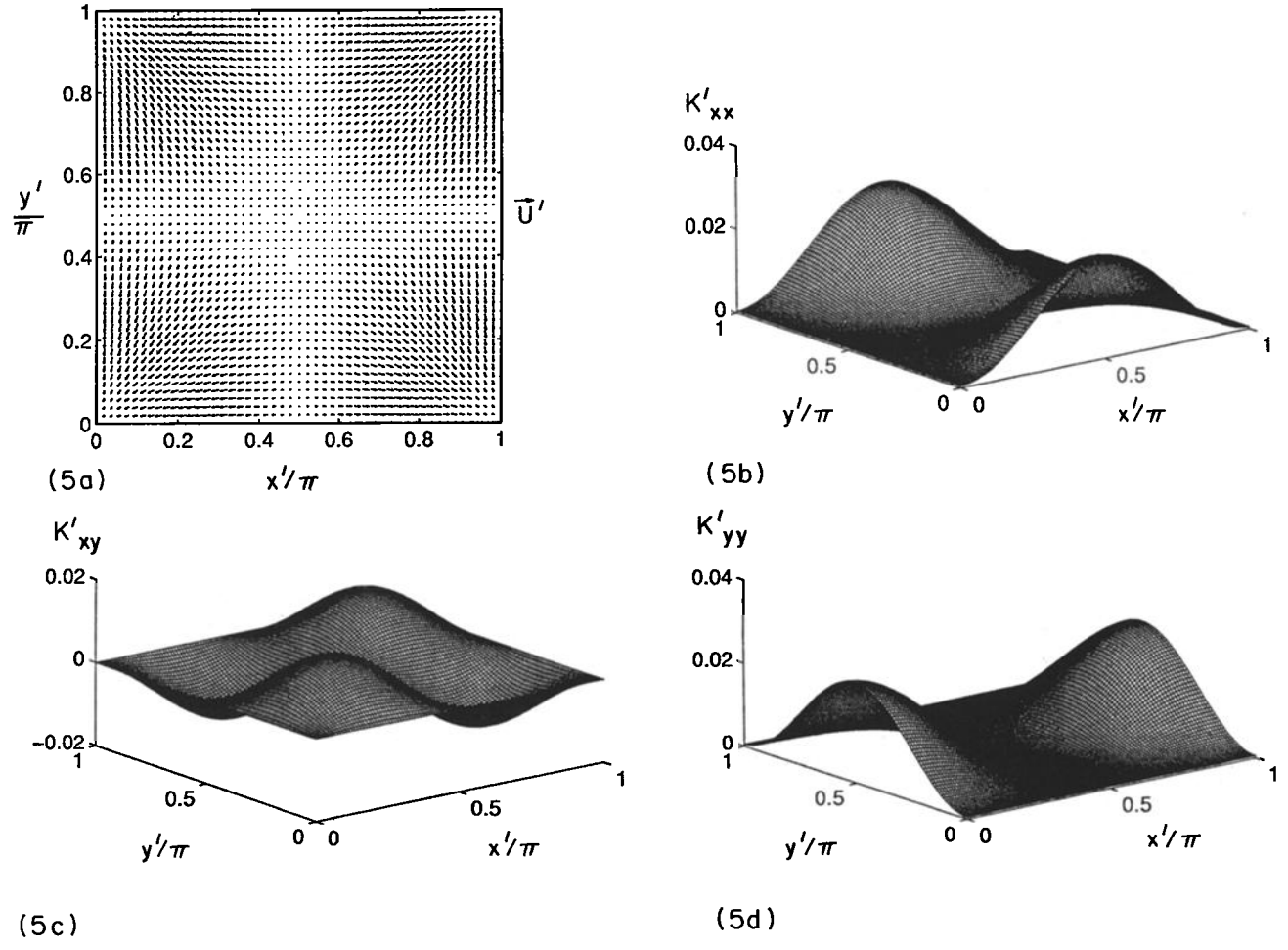

Figure 5. Seiche mode $n = m = 1$. (a) Weighted depth average of convection veocity, (b) K'_{xx}, (c) K'_{xy}, (d) K'_{yy}, with $K'_{ij} = D\delta_{ij} + \mathcal{D}_{ij}$.

ter is erodible (similar to Okeechobee Lake in southern Florida); the normalized side of the rectangle is $\pi/4$. For each lake the same modes of standing waves are studied.

The first mode $m = n = 1$ has been studied by Mei and Chian for a nonerodible bed. The convection field converges to the four corners, see Figure 5 a. The dispersion coefficients are shown in Figures 5 b-5d. We display the erosion rates for Lake A in Figure 6 and Lake B in Figure 7. As shown in Figure 8, resuspended sediments in Lake A first build up a plateau directly over the area of erosion. Some of the particles resuspended from the coastal belt are convected toward the corners. This accumulation implies that the sediment concentration will undergo upwelling in a boundary layer next to the vertical cliff near the corners. This tendency will

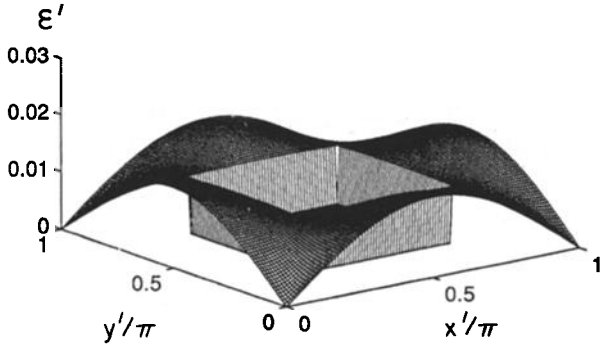

Figure 6. Seiche mode $n = m = 1$. Erosion rate over a lake where the coastal strip is erodible.

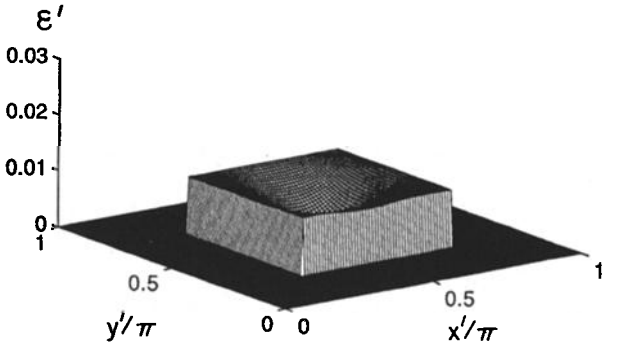

Figure 7. Seiche mode $n = m = 1$. Erosion rate over a lake where the center part is erodible.

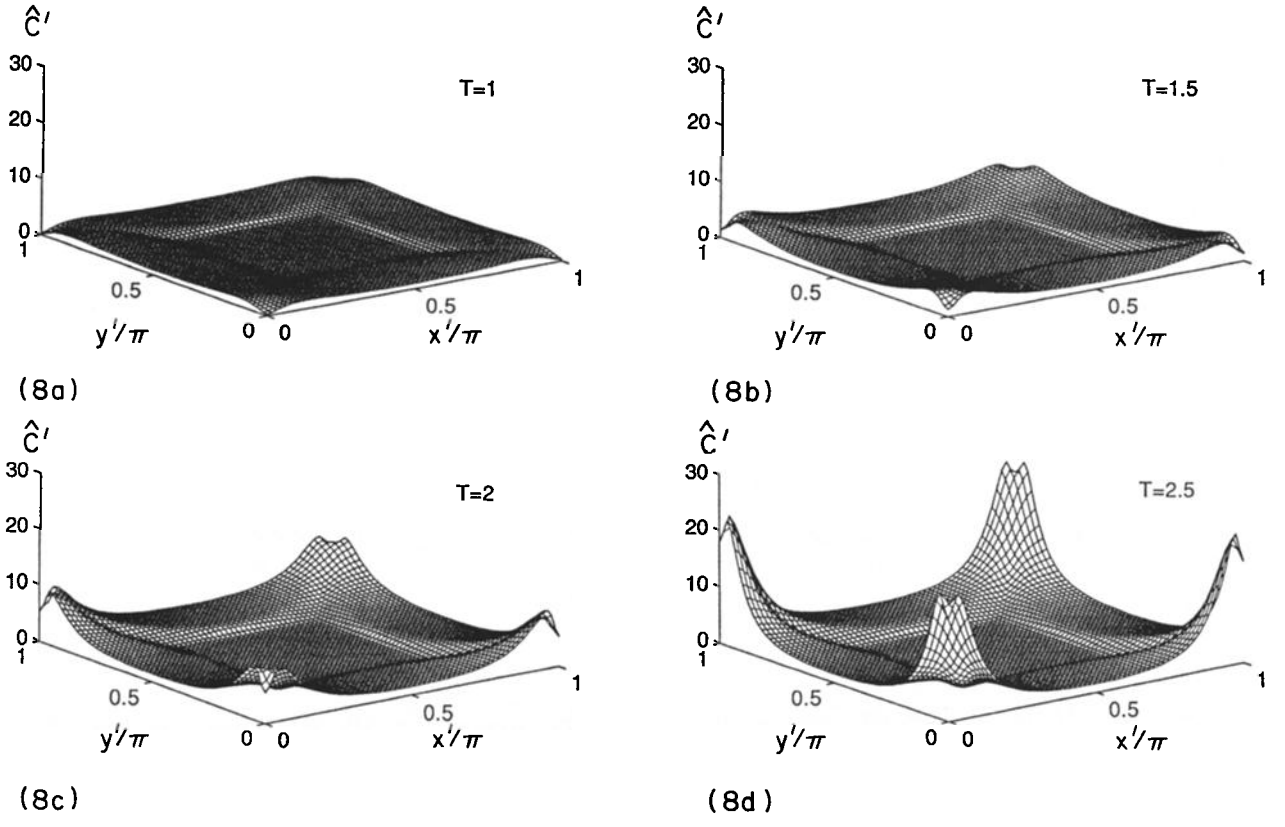

Figure 8. Seiche mode $n = m = 1$. Evolution of bottom concentration due to erosion along the coastal strip.

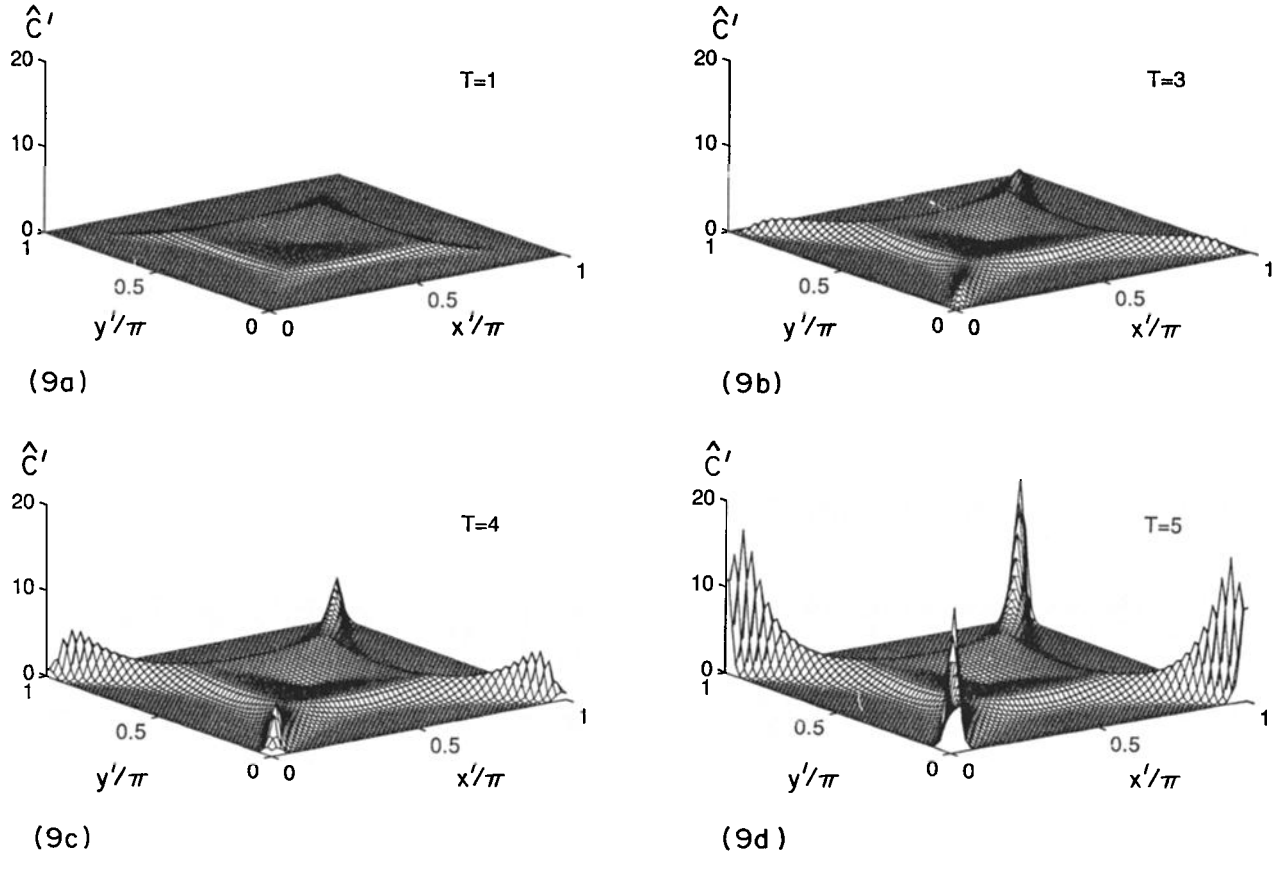

Figure 9. Seiche mode $n = m = 1$. Evolution of bottom concentration due to erosion over the center.

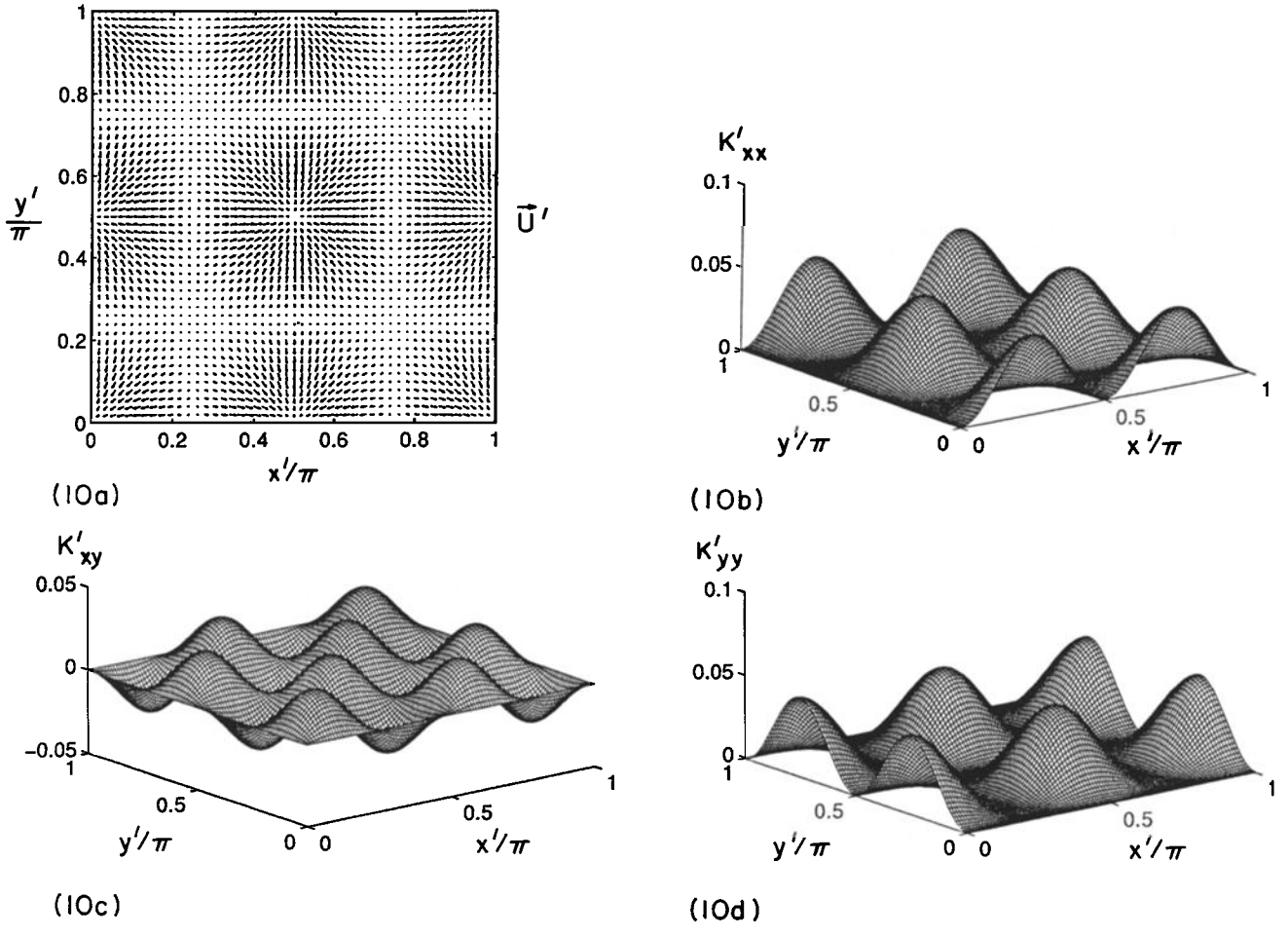

Figure 10. Seiche mode $n = m = 2$. (a) Weighted depth-average of convection veocity, (b) K'_{xx}, (c) K'_{xy}, (d) K'_{yy}, with $K'_{ij} = D\delta_{ij} + \mathcal{D}_{ij}$.

be limited, of course, by the eventual attenuation of the waves in reality. In Lake B the particles eroded from the center are transported across the non-erodible coast toward the four corners, as shown in Figure 9. To have some quantitative ideas, we take a lake of size $a = b = 10\,km, h = 10\,m$. The first mode has the eigenfrequency $\omega = \sqrt{2}\pi \times 10^{-3}\,rad/s$, or eigenperiod of $\sqrt{2} \times 10^3\,s$. The wave number is $k = \omega/\sqrt{gh} = \sqrt{2}\pi \times 10^{-4}\,m^{-1}$. For a wave amplitude of $A = 0.2\,m$ the bottom velocity scale is $U_b = 0.1\,m/s$. The scale of bed stress is $\tau_o = 0.42\,N$ according to (84). The time scale of convection is $\omega/k^2U_b^2 = (\sqrt{2}\pi)^{-1} \times 10^7 s = 26$ days. Thus the predicted phenonmena are relevant in winter months when waves may persist sufficiently long.

For the higher mode with $n = m = 2$, the distributions of convection velocity and dispersion coefficients in mode $(n = m = 1)$ are repeated in four quadrants as shown in Figure 10. Therefore, five more points of convergence are added at the center of the lake and the center of the four coasts. The erosion rate distributions in Lakes A and B are shown in Figures 11 and 12. At large times accumulations occur at eight points along the coasts, as shown in Figure 13. In Lake B there are now interior points of convergence including the center of the lake; final buildup at the center is the most prominant, as can be seen in Figure 14.

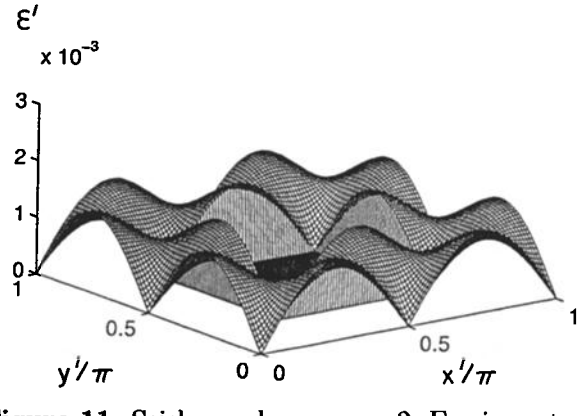

Figure 11. Seiche mode $n = m = 2$. Erosion rate over a lake where the coastal strip is erodible.

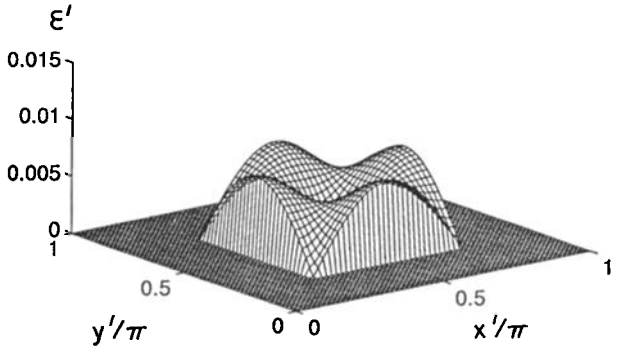

Figure 12. Seiche mode $n = m = 2$. Erosion rate over a lake where the center part is erodible.

Concluding Remarks

In this paper we have demonstrated the total dynamical effects of waves on the resuspension as well as the transport of fine sediments. By excluding currents associated with tides or wind-induced circulation, we have examined for several examples the influence of the wave pattern on the transport of suspended sediments. Deposition is neglected. In our examples the wave pattern has a strong influence on the erosion and transport of suspended sediments. Since the current induced by waves can be as strong as that of tides or of the mean wind, future theories should not relegate waves to the simple role of augmenting the bottom shear stress and affecting the rate of erosion alone. An accurate prediction of waves, with regard to their generation and maintainence by wind, their dissipation by bottom friction and whitecapping, and their refraction and diffraction, is a prerequisite for the prediction of sediment dynamics. The effects of waves on the erosion, convection and diffusion of fine particles must be combined with those of the current due to the mean wind and tides. *Madsen* [1978] showed that the drift current near the sea surface with wind and waves is not the sum of Stokes drift by waves and the Ekman drift by the mean wind. In view of this theory, radiation stresses across the depth of a shallow sea must interact with Ekman drift to help the horizontal transport of suspended sediments.

In addition to sediment resuspension which is of interest to the transport of nutrients and contaminants in lakes and coastal waters, waves can also move the highly concentrated fluid mud which is known to behave as a non-Newtonian fluid. In return waves are attenuated by supplying energy for dissipation in fluid mud [*Mei and Liu*, 1987; *Liu and Mei*, 1989; 1993, *Jiang*, 1993; *Jiang and Mehta* , 1992]. Clearly there is a need for a theoretical model emcompassing the coupled movement of

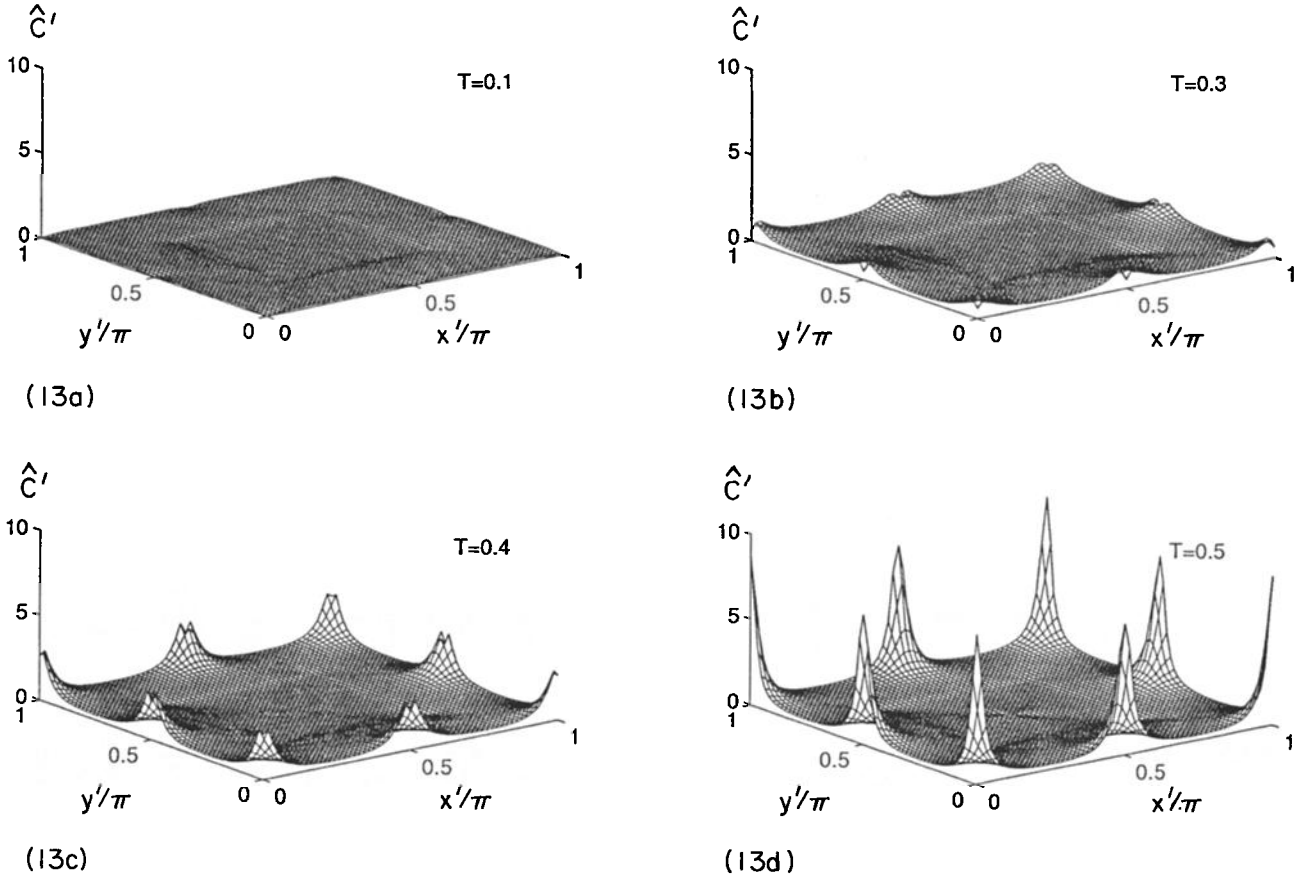

Figure 13. Seiche mode $n = m = 2$. Evolution of bottom concentration due to erosion along the coastal strip.

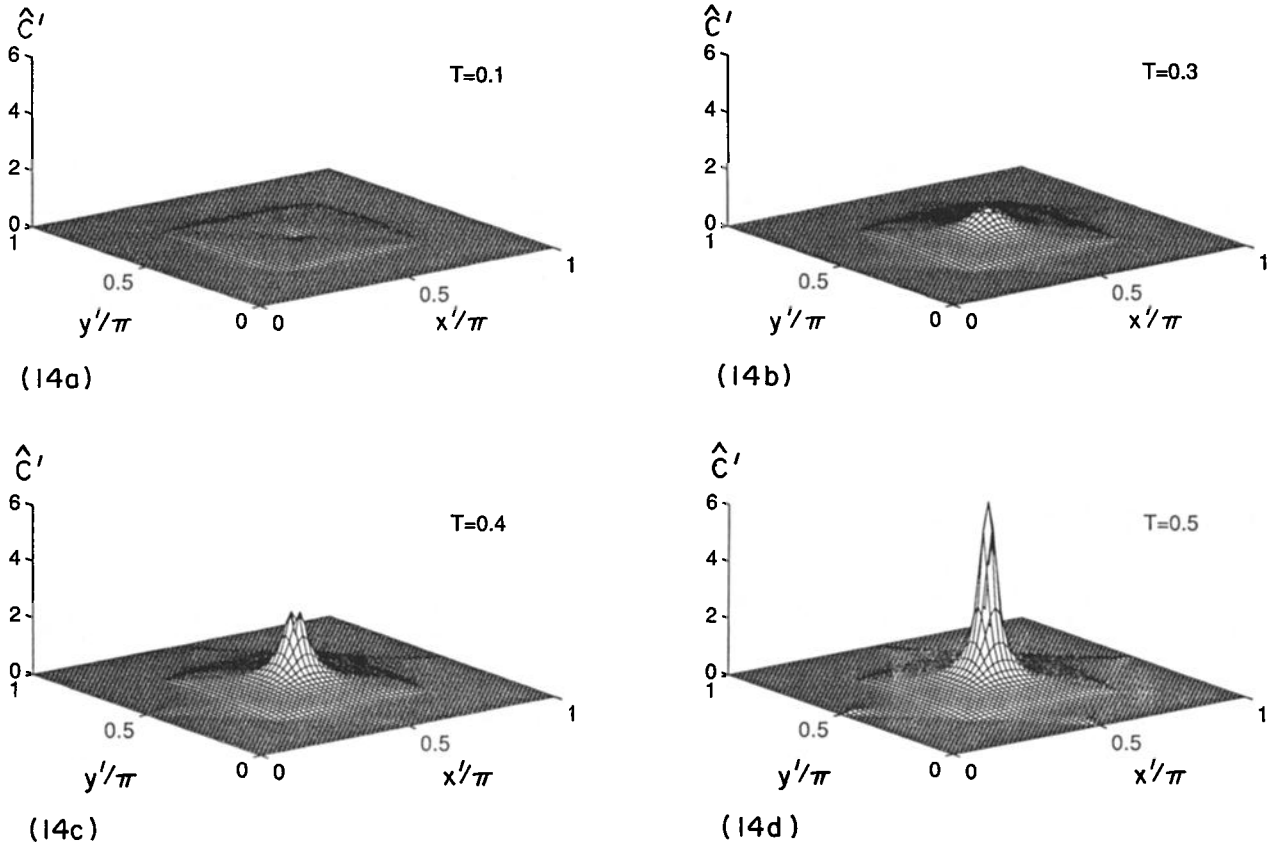

Figure 14. Seiche mode $n = m = 2$. Evolution of bottom concentration due to erosion over the center.

wind, waves and fluid mud, as well as the erosion and deposition of sediments near the bottom.

Acknowledgments. The authors are grateful for funding provided by the U. S. Office of Naval Research (grant N00014-89-J-3128, Ocean Technology Program directed by Thomas Swean), and by the U. S. National Science Foundation (grant CTS-9634120, Fluids, Hydraulics and Particulates Program directed by Roger Arndt), State Key Laboratory for Estuarine and Coastal Research, East China Normal University, and the South Florida Water Management District. We also thank the referees for some perceptive comments.

References

Horikawa, K., and A. Watanabe, *Nearshore Dynamics and Coastal Processes.* Univ. of Tokyo Press, Tokyo 1988.

Huhe, O., and Yang, M.Q. Experimental study of the properties of cohesive sediment of the Yellow River Delta. Report (in Chinese), p. 39, by the Insts Mech., Chinese Acad. of Sci., 1996.

Jiang, F., Bottom mud transport due to water waves, Ph. D. thesis, 222 pp., Univ. of Fl., Gainsville, 1993.

Jiang, F. , and A. J. Mehta, Some observations on fluid mud respsonse to water waves, in *Dynamics and Exchanges in Estuaries and the Coastal Zone, Coastal and Esturies Stud. Ser.* vol. 40, edited by D. Prandle, pp. 351-376, AGU, Washington, D. C., 1992.

Koman, G.L., L. Caverleri, M. Donelan, K. Hasselmann, S. Hasselmann, and P.A.E.M. Janssen, *Dynamics and Modelling of Ocean Waves.* Cambridge Univ. Press, New York 1994.

Krone, R.B., Flume studies of the transport of sediment in estuarial shoaling processes, 110 pp, Univ. of Calif. Hydraul. Eng. and Sanitary Eng. Res. Lab, Berkeley, Calif. 1962.

Liu, K. F. , and C. C. Mei, Effects of wave-induced friction on a muddy seabed modelled as a Bingham- plastic fluid. *J. Coastal Res., 5* (4) 777-789, 1989.

Liu, K. F. , and C. C. Mei, Long waves in shallow water over a layer of Bingham-plastic fluid-mud, I. physical aspects. *Int. J. Eng. Sci. 31,* 125-144, 1993.

Luettich, R.A., D.R.F. Harleman, and L. Somlyódy, Dynamical behaviour of suspended sediment concentrations in a shallow lake perturbed by episodic wind stress. *Limnol. Oceanogr. 35,* 1050-1067, 1990.

Madsen, O.S., Mass transport in deep-water waves,*J. Phys. Oceanogr. 8,* 1009-1015, 1978.

Mehta, A. J., Characterization of cohesive sediment properties and transport processes in estuaries, in *Estuarine Cohesive Sediment Dynamics* edited by A. Mehta, pp. 290-325, Springer-Verlag, New York, 1984 .

Mehta, A.J. and E. Patheniades, Resuspension of deposited cohesive sediment beds, *Coastal Eng.*, 1569-1588, 1982.

Mei, C.C. and C.M. Chian, Dispersion of small suspended particles in a wave boundary layer, *J. Phys. Oceanogr., 24,* 2479-2495, 1994.

Mei, C. C., and K. F. Liu, A Bingham-plastic model for a muddy seabed under long waves, *J. Geophys. Res. 92* (C13), 14,581-14,594, 1987.

Patheniades, E., Erosion and deposition of cohesive soils. *J. Hydraul. Div. Amer. Soc. Civ., Engrs. 91* (HY1)., 105-139, 1965.

Sanford, L.P., Wave-induced resuspension of upper Chesapeake Bay muds. *Estuaries, 17*, 148-165, 1994.

Sheng, Y.P., Modeling bottom boundary layer and cohesive sediment dynamics in estuarine and coastal waters. *Estuarine Cohesive Sediment Dynamics* edited by A. Mehta, 360-400, Springer-Verlag, New York, 1984.

Sheng, Y.P. and X. Chen, A three-dimensional numerical model of hydrodynamics, sediment transport and phosphorus dymamics in Lake Okeechobee: Theory, model development and documentation, *Report C91-2393*, Univ. of F. Coastal and Oceanogr. Eng. Lab., Gainsville, 1991.

Sheng, Y.P., and V. Cook, Resuspension and vertical mixing of fine sediments in shallow water, Part B. *Report C90-020*, Univ. of Fl. Coastal and Oceanogr. Eng. Lab., Gainsville, 1990.

Sheng, Y.P., and W. Lick, The transport of resuspension of sediments in shallow lakes, *J. Geophys. Res., 84*, 1809, 1979.

Sheng, Y. P., D. E. Eliason, J. K. Choi, X. Chen, and H. K. Lee, Effect of sediment resuspension on numerical simulation of three-dimensional wind-driven circulation and sediment transport in Lake Okeechobee during spring 1989. *Report 91-019* Univ. of Fl. Coastal and Oceanogr. Eng. Lab., GAinsville 1991.

Sleath, J.F.A. Seabed boundary layers. in *The Sea* Vol. 9, Part B, edited by B. Le Mehaute and D.M. Hanes, pp. 693-727, Wiley-Interscience, New York, 1990.

Sobey, R., Wind-wave prediction *Ann. Rev. of Fluid Mech., 18*, 149-172, 1986.

Trowbridge, J. and O. S. Madsen, Turbulent wave boundary layers. 1. Model formulation and first- order solution. *J. Geophys. Res., 89* (C5), 7989-7997, 1984a.

Trowbridge, J. and O. S. Madsen, Turbulent wave boundary layers. 2. Second-order theory and mass transport. *J. Geophys. Res.. 89* (C5), 7999-8007, 1984b.

van Rijn, L.C., *Principles of Sediment Transport in Rivers, Estuaries, and Coastal Seas*, Aqua Publ,. Amsterdam, 1994.

Yu, K. H., Preliminary study for the planning of Zhongshan Harbor, Jian Su Province. (in Chinese), *Internal Rep. 9406*, Rivers and Harbors Res. Inst., Nanjing, China, 1993.

C. Mei, Department of Civil and Environmental Engineering, Massachusetts Institute of Technology, Cambridge, MA, 02139. (e-mail: ccmei@mit.edu)

S. Fan, Department of Ocean Sciences, Old Dominion University, Norfolk, VA, 23508. (e-mail: sjfan@ocean.odu.edu)

K. Jin, South Florida Water Management District, West Palm Beach. FL, 33406. (e-mail: kang-ren.jin@sfwmd.gov)

(Received September 20, 1996; revised January 15, 1997; accepted January 23, 1997.)